Journal of Hazardous Materials 404 (2021) 123700

Contents lists available at ScienceDirect

Journal of Hazardous Materials

journal homepage: www.elsevier.com/locate/jhazmat

Methylmercury biomagnification in aquatic food webs of Poyang Lake, China: Insights from amino acid signatures

Zhongyi Zhang [a], Wen-Xiong Wang [b,c], Nengjian Zheng [a], Yansheng Cao [a], Hongwei Xiao [a], Renguo Zhu [a], Hui Guan [d], Huayun Xiao [a,*]

[a] Jiangxi Province Key Laboratory of the Causes and Control of Atmospheric Pollution, East China University of Technology, Nanchang, 330013, China
[b] Research Centre for the Oceans and Human Health, City University of Hong Kong Shenzhen Research Institute, Shenzhen, 518057, China
[c] School of Energy and Environment, State Key Laboratory of Marine Pollution, City University of Hong Kong, Kowloon, Hong Kong, China
[d] The State Key Laboratory of Environmental Geochemistry, Institute of Geochemistry, Chinese Academy of Sciences, Guiyang, 550081, China

ARTICLE INFO

Editor: R Sara

Keywords:
MeHg
Cysteine
Compound-specific nitrogen isotope of amino acid
Biomagnification
Poyang Lake

ABSTRACT

As the dominant mercury species in fish, methylmercury (MeHg) biomagnifies during its trophic transfer through aquatic food webs. MeHg is known to bind to cysteine, forming the complex of MeHg-cysteine. However, relationship between MeHg and cysteine in large-scale food webs has not been explored and contrasted with MeHg biomagnification models. Here, we quantified the compound-specific nitrogen isotopic analysis of amino acids (CSIA-AA), MeHg, and amino acid composition in aquatic organisms of Poyang Lake, the largest freshwater lake in China. The trophic positions (TP_{AA}) of organisms ranged from 1.0 ± 0.1–3.7 ± 0.2 based on CSIA-AA approach. The trophic magnification factor (TMF) of MeHg, derived from the regression slope of Log-transformed MeHg in organisms upon their TP_{AA} for the entire food web was 9.5 ± 0.5. Significantly positive regression between MeHg and cysteine ($R^2 = 0.64$, $p < 0.01$) was documented, suggesting MeHg-cysteine complex may potentially play a critical role in the bioaccumulation of MeHg. Furthermore, TMFs of MeHg calculated with and without cysteine normalization compared well (7.7–8.7) when excluding primary producers. Our results implied that MeHg may biomagnify as the complex of MeHg-cysteine and contribute to our understanding of MeHg trophic transfer at the molecular level.

1. Introduction

Mercury (Hg) is a globally distributed semi-volatile pollutant, and is released to the atmosphere via both natural (e.g., volcanoes, biomass burning) and anthropogenic processes (e.g., gold mining, fossil fuel combustion, metal smelting, and cement production; Pirrone et al., 2010; Selin, 2009). More than 90 % of Hg released to the atmosphere is elemental Hg (Hg^0), which has a long atmospheric lifetime (0.5–2 years) and is ultimately removed from the atmosphere through (1) oxidation to Hg^{2+} by ozone, hydroxyl radical and halogen radicals, or (2) uptake by vegetation (Driscoll et al., 2013; Pirrone et al., 2010; Selin, 2009). Once deposited in terrestrial and aquatic ecosystems, Hg is susceptible to transformation to MeHg, a bioaccumulative neurotoxin (Schaefer and Morel, 2009; Yin et al., 2017; Li et al., 2016). Because of its high biomagnification potential, considerable levels of MeHg have been observed in various top predators, even those inhabiting in remote areas (Fox et al., 2017; Ruus et al., 2015). Consumption of fisheries products is therefore regarded as the primary MeHg exposure pathway for the global human population.

MeHg accounts for the majority of THg in fish muscle (Abeysinghe et al., 2017; Lescord et al., 2018; Sackett et al., 2015) and can be biomagnified efficiently along the aquatic food webs, reaching concentrations millions of times higher in wildfish than in the surrounding water (Blum et al., 2013; Clayden et al., 2013; Yin et al., 2016). Ecosystem characteristics (e.g., pH, nutrient, temperature) and food web processes (e.g., species diversity, growth rate) are known to affect the biomagnification of MeHg, while trophic transfer remains the primary driver (Clayden et al., 2013; Lavoie et al., 2013). Trophic transfer of MeHg in aquatic food webs is closely coupled to the metabolism (e.g, subcellular distribution, assimilation efficiency) of MeHg (Adediran et al., 2019; Wang, 2012). Dang and Wang (2010) observed that the bioavailability of MeHg associated with different subcellular fractions (e.g., heat-stable protein, cellular debris) was comparable due to high assimilation efficiencies (90–94 %). Furthermore, MeHg has been shown

* Corresponding author.
E-mail address: xiaohuayun@ecut.edu.cn (H. Xiao).

https://doi.org/10.1016/j.jhazmat.2020.123700
Received 20 May 2020; Received in revised form 16 July 2020; Accepted 8 August 2020
Available online 18 August 2020

to conjugate with cysteine as the complex of MeHg-cysteine, and as a result accumulates in fish muscle protein (Harris et al., 2003; Lemes and Wang, 2009; Leaner and Mason, 2002). MeHg transportation across the cellular membrane, such as during the digestive processes of fish, is also mediated via the complexes of MeHg-cysteine because this complex is a structural mimic of the essential amino acid methionine, which is a substrate for amino acid carriers such as the L-type neutral amino acid transporters (LATs; Leaner and Mason, 2002; Simmons-Willis et al., 2002). A few earlier studies also suggested that the trophic transfer of MeHg may be exclusively in the form of MeHg-cysteine (Simmons-Willis et al., 2002; Thera et al., 2019; Leaner and Mason, 2002). However, the effects of amino acid metabolism, especially essential amino acids cysteine and methionine, on the prey-predator relationships and the trophic transfer of MeHg, has been rarely explored and warrants further investigation.

The trophic magnification factor (TMF), derived from the slope of a Log-normal regression of contaminants (e.g., MeHg) in organisms upon their corresponding trophic positions (TPs) has been widely used to assess the average trophic transfer of Hg across food webs (Borgå et al., 2012; Burkhard et al., 2013; Ek et al., 2018). Analysis of bulk stable nitrogen isotope ($\delta^{15}N_{Bulk}$) in biota provides a continuous measure of the relative position of organisms within a food web (Hussey et al., 2014). However, this approach has a few limitations that can introduce considerable uncertainty into a TMF study (Borgå et al., 2012; Post, 2002). Firstly, both MeHg and $\delta^{15}N_{Bulk}$ in aquatic organisms are affected by the availability and composition of protein (i.e., amino acid composition; Clayden et al., 2013; Karimi et al., 2007; Robbins et al., 2010; Man et al., 2019). For example, the variability of MeHg in aquatic invertebrates is related to their tissue content of cysteine (Thera et al., 2019). Secondly, the trophic ^{15}N-enrichment factor ($\Delta^{15}N$, approximated 3.4‰ at each shift of TP), is known to be affected by protein quality and shows a high variation with different species, physiology, and trophic ecology (Robbins et al., 2010, Zanden and Rasmussen. 2001). For instance, the $\Delta^{15}N$ values among different animals (i.e., insects, mammals) exhibited considerable variations (e.g., −0.5‰ to +9.2‰; Post, 2002; Zanden and Rasmussen, 2001). Another limitation is the spatial and temporal variations in the nitrogen isotope baseline of the ecosystem in question (Ek et al., 2018; Lorrain et al., 2015). A common solution has been to use the long-lived primary consumer as TP of 2.0 (Zanden and Rasmussen, 2001), but recent studies indicated that these long-lived primary producers may be omnivorous, and their isotopic compositions were also variable both temporally and spatially (i.e., in-depth; Chikaraishi et al., 2014; Choi et al., 2017; Cummings and Schindler, 2013; Matthews and Mazumder, 2003). Therefore, a better understanding of the food web structure is critical for accurate TMF assessments (Borgå et al., 2012; Kidd et al., 2001). Moreover, TMF was used to quantify the trophic transfer of contaminants rather than the relative change of the associated cellular medium (Borgå et al., 2012; Burkhard et al., 2013). Therefore, whether MeHg should be normalized by the cellular medium such as proteins remains to be resolved. To the best of our knowledge, the relationship between MeHg and cysteine or protein has only been rarely explored and contrasted to MeHg biomagnification models based on TPs.

To establish reliable and accurate estimation of TP, the compound-specific nitrogen isotopic analysis of amino acid (CSIA-AA) has been regarded as a promising measure (Chikaraishi et al., 2014, Ek et al., 2018). The most significant advantage of the CSIA-AA approach is that it defines the TP upon the basis of the metabolic pathways of amino groups of amino acids (Mcmahon and Mccarthy, 2016; O'Connell, 2017; Steffan et al., 2015). Specifically, the trophic amino acids are highly ^{15}N-enriched during transamination as the cleavage of C—N bonds, while source amino acids show little changes in their $\delta^{15}N$ values during metabolic processes since the carbon-nitrogen bonds (C—N) are neither formed or cleaved. Therefore, heavily fractionated trophic amino acids (e.g., glutamate, enriched by +8.0‰) provide a robust indicator of trophic step, while less fractionated source amino acids (e.g., phenylalanine and methionine, enriched by +0.4‰ and +0.5‰, respectively) closely mirror the nitrogen isotope baseline at the base of the food web (Chikaraishi et al., 2009). Accordingly, the CSIA-AA approach produces a more accurate and precise estimation of the TP compared to other methods (Chikaraishi et al., 2014; Steffan et al., 2015).

In this study, we measured the amino acid nitrogen isotopic composition, amino acid contents (particularly cysteine), and the corresponding contents of THg and MeHg in organisms collected from the Poyang Lake, the largest freshwater lake in China. TMF was examined under several scenarios, i.e., with or without normalization by protein or cysteine; with or without consideration of primary producers to clarify their influences. Our objectives were: 1) to examine whether the MeHg concentrations of organisms were related to their protein or cysteine contents; 2) to compare TPs inferred from bulk and CSIA-AA approach (TP_{Bulk} vs TP_{AA}); finally 3) to reveal the differences between the TMFs derived from traditional bulk $\delta^{15}N$ approach and CSIA-AA approach.

2. Materials and methods

2.1. Field sample collection and processing

As the largest freshwater lake of China, Poyang Lake covers an area of 3283.41 km^2 (average depth of 8.4 m) and provides significant environmental benefits to China in terms of supplying water resources and maintaining carbon storage and biodiversity. In October 2016, aquatic organisms of food web components were systematically sampled from the southern area of Poyang Lake (28°48′N~29°05′N, 116°22′E~116°29′E, Fig. S1), following a previous protocol (Zhang et al., 2019). These samples included four representative primary producers (including algae, n = 3; terrestrial C3 input, n = 3; aquatic macrophyte, n = 8; and particulate organic matter, n = 3), two abundant macrobenthic species (filter-feeding mussel of *Hyriopsis cumingii*, n = 5 and surface-grazing snail of *Cipangopaludina cahayensis*, n = 4), omnivorous shrimp (*Macrobrachium nipponensis*, n = 3; *Procambarus clarkia*, n = 4), one crab (*Eriocheri sinensis*, n = 3) and 27 fish species (i.e., herbivore: *Parabramis pekinensis* and *Ctenopharyngodon idellus*; planktivore: *Hemiculter leucisculus*, *Tylosurus melanotus* and *Hemibarbus maclatus*; carnivores: *Silurus asotus* and *Siniperca chuatsi*; detritivore: *Parabotia fasciata* and omnivores.

n = 103 for fish species). Detailed information on the species, numbers of the sample, and feeding habits are summarized in Table 1 and Text S4.

Briefly, fish, shrimps, and crabs were sampled with the help of local fishermen using homemade trawl, fixed nets, and casting nets, while snails and freshwater mussels were collected using homemade trawl. These samples were kept on ice-bag and immediately transported to the laboratory. Primary producers, represented by terrestrial input (*Phragmites australis* and *Artemisia igniaria*), aquatic macrophytes, and algae, were collected at the same time. Leaves of terrestrial plants were collected by hand, while attached algae were scraped gently off the plants and stones. Samples of particulate organic matter (POM) were obtained by filtering 2 L of surface water onto pre-combusted glass GF/C filter (Whatman, 1.2 μm pore size). In the laboratory, all samples were sorted into major taxa and rinsed with 18.2 MΩ•cm water (Millipore).

The dorsal muscle was collected from large fish after removing the skin and scales. The whole body was taken from small fish to obtain a sufficient sample amount. For invertebrates (e.g., shrimp, mussel), the shell was removed and the pooled muscle tissues were used for analysis. POM samples were acidified using 1 mol/L HCl to remove possible carbonate contamination. These acidified samples (POM) were used for the bulk $\delta^{13}C$ analysis, and the untreated samples were used for the $\delta^{15}N$ analysis. All the samples were freeze-dried, homogenized, and subsampled for analysis (isotopic composition, THg, MeHg, and amino acid concentrations).

2.2. THg and MeHg analysis

THg concentrations of all freeze-dried samples were determined using a Direct Mercury Analyzer (Milestone, DMA-80) according to USEPA 7473 Method (EPA, 2002). MeHg analysis followed a previous protocol (Liang et al., 2003). Briefly, about 200 mg of the freeze-dried sample was mixed with 3 mL 25 % (W/V) KOH (in CH_3OH) in a 50-mL centrifuge tube and shaken mechanically for 12 h. Then, 3 mL of 6 mol/L HCl, 4 mL of acidic $KBr/CuSO_4$ (3:1), and 5 mL of CH_2Cl_2 were added into the tube in sequence and shaken for 2 h to extract the MeHg into the organic phase. Following centrifugation at 2000 rpm for 10 min, the organic phase was transferred into a 10-mL glass tube and extracted with 1 mL sodium thiosulfate. After extraction, the water phase was pipetted and injected directly into the HPLC-AFS system for separation and determination (Liang et al., 2003).

A certified reference material (GBW10029, n = 15) and 20 randomized replicate samples were analyzed for quality assurance/quality control protocols (QA/QC) of THg and MeHg. The method detection limit for MeHg was better than 0.5 ng/g. The mean recoveries of THg and MeHg for the reference material were 102 ± 5% (mean ± SD) and 97 ± 5%, respectively, and the relative standard deviation of THg and MeHg for replicate samples was typically < 10 %. The variation coefficients for the analysis of MeHg and THg for the replicate samples were less than 12 %.

2.3. Amino acid concentrations

Analysis of proteinaceous amino acid (AA) composition followed a method reported previously (Manneberg et al., 1995). Briefly, 5.00 mg of sample was hydrolyzed with 6 mol/L HCl at 110℃ in the presence of 0.02 % phenol (W/V). To quantify the cysteine content, every sample was hydrolyzed twice, with and without oxidation. Both cysteine and cystine residues in protein were oxidized into cysteic acid following hydrolysis in the presence of sodium azide (NaN_3, 0.20 %, W/V), and the content of cysteine was equal to the concentration difference between cysteic acid (hydrolysis with NaN_3) and cystine (without NaN_3). The amino acid composition of both set samples was determined using the amino acid analyzer (A300, Membrapure). A total of 19 AAs (cysteine, cystine, methionine, aspartate, arginine, glycine, valine, leucine, isoleucine, phenylalanine, threonine, lysine, histidine, tyrosine, glutamate, serine, threonine, alanine, proline) were determined. Generally, the 19 AAs were linear from 0.1–5 nmol ($R^2 > 0.99$), with a method detection limit of better than 20 pmol. The recovery for every AA was better than 95 %. Bovine serum albumin (BSA) was used to assess the oxidation efficiency for the conversation of cysteine to cysteic acid. The BSA hydrolysis in the presence of 0.20 % NaN_3 normally resulted in 93–100 % oxidation of cysteine to cysteic acid. The protein content was then calculated as the total of determined hydrolyzed AAs. Further information is provided in the Text S1.

2.4. Isotopic analysis

Bulk C and N isotopic analyses were carried out on the freeze-dried samples using an elemental analyzer–isotope ratio mass spectrometer (EA-IRMS, Flash 2000 and MAT253 Plus, Thermo Fisher Scientific Inc., USA) following a previous method (Zhu et al., 2018). Based on replicates of laboratory standards, the analytical precisions for $\delta^{13}C$ and $\delta^{15}N$ were better than 0.1‰.

The CSIA-AA was conducted using a previously described method (Zhang et al., 2016). Individual AAs were firstly converted to N-pivaloyl/isopropyl ester derivatives according to a modified protocol (Chikaraishi et al., 2009), and the $\delta^{15}N$ values were then determined via a Delta V mass spectrometer equipped a Trace GC Ultra (GC Isolink + ConFlo IV, equipped with an Agilent DB-5 ms column) to obtain a baseline separation of the AA mixtures (Zhang et al., 2016). To assess the isotopic analysis reproducibility, amino acid reference mixtures with known $\delta^{15}N$ values were analyzed after every five sample runs. Each sample was analyzed in triplicate, and the intensity of most elution peaks was kept higher than 400 mV to obtain an associated analytical error of typically < 1.0‰. Further details on the lab analyses and quality assurance procedures (i.e., bulk isotope, CSIA-AA) are provided in the Text S2, S3.

2.5. Trophic position and statistical analyses

The TP values based on CSIA-AA and bulk isotope approach were calculated using the following equation (Chikaraishi et al., 2009; Zhang et al., 2019), respectively. For TP_{AA} calculation, trophic enrichment factor (TEF) at each shift of TP was set as 7.6 ± 1.2‰ (Chikaraishi et al., 2009). The β_{mix} is the averaged difference between $\delta^{15}N_{Glu}$ and $\delta^{15}N_{Phe}$ of the lake primary producers digested by an individual consumer. $\beta_{vascular}$ value for terrestrial vascular and aquatic plants (i.e., +8.4 ± 1.6‰) is higher than that for aquatic algae, eukaryotic and prokaryotic photoautotrophs (β_{algae}, −3.4 ± 0.9‰) (Chikaraishi et al., 2009; Yamaguchi et al., 2017). Therefore, β_{mix} for an individual was first calculated based on their dietary composition to accurately estimate their TP_{AA}:

$$\beta_{mix} = \beta_{vascular} \times f + \beta_{algae} \times (1\text{-}f) \quad (1)$$

$$TP_{AA} = [(\delta^{15}N_{Glu} - \delta^{15}N_{Phe} - \beta_{mix})/TEF] + 1 \quad (2)$$

The $\delta^{15}N_{Glu}$ and $\delta^{15}N_{Phe}$ are the $\delta^{15}N$ values of glutamate and phenylalanine, respectively. The *f* and 1-*f* represent the relative contributions of vascular resources (terrestrial input and aquatic plants) and algae for each consumer, respectively, which can be calculated using a Bayesian mixing model (simmr; Text S4, Parnell et al., 2013). By explicitly accounting for several uncertainties (i.e., multiple sources, fractionation factors, and determined isotopic signatures), the simmr model can determine the probability distribution of source contributions to a mixture. Multiple isotopic tracers ($\delta^{15}N$, $\delta^{13}C$, $\delta^{15}N_{Glu}$, $\delta^{15}N_{Phe}$) were employed to improve the performance of simmr (Zhang et al., 2019). Detailed information about the simmr model was provided in Text S4.

For estimation of TP_{Bulk}, a representative $\Delta^{15}N$ was used as the average trophic shift (i.e., 3.4‰) and average $\delta^{15}N$ values of long-lived primary consumers (i.e., freshwater mussels) as a baseline (Post, 2002).

$$TP_{Bulk} = (\delta^{15}N_{consumer} - \delta^{15}N_{baseline}) / \Delta^{15}N + 2 \quad (3)$$

The MeHg concentrations were logarithm-transformed for statistical analysis to meet the assumptions of normality and equal variance. The trophic magnification factors (TMFs, and the potential uncertainty considering the propagation of uncertainty of slope "b") were calculated as the antilog of the regression slope (to the base 10 in this study) of the MeHg concentration against the TP (both TP_{Bulk} and TP_{AA}, Text S4) :

$$Log_{10}[MeHg] = a + b \times TP \quad (4)$$

$$TMF = 10^b \quad (5)$$

Multiple linear regression analyses using protein, cysteine content, $\delta^{15}N_{Bulk}$, and TP_{AA} of food web organisms were conducted to examine whether protein or cysteine content explained additional variation in Log MeHg concentrations. An Akaike Information Criterion (AIC) adjusted for small sample sizes (AIC_c) was used to identify the best model (Anderson and Burnham, 2004). Usually, the lower AIC_c means the better of the model (Text S5). The variance inflation factor (VIF), which was used to test the multicollinearity between independent variables, were generally less than 2 among the examined independent variables in this study (Table S4, Text S5).

Analysis of variance (ANOVA) was used to compare the differences in TP for each species between the estimation approaches (TP_{AA} vs TP_{Bulk}). The slopes in Eq. (4) among different scenarios (with and without primary producers, before and after normalization with

cysteine or protein) and between the bulk and CSIA-AA methods were compared using analysis of covariance (ANCOVA). Specific comparisons of MeHg biomagnification through the pelagic and benthic food webs were also conducted using ANCOVA. Alpha was set to 0.05 in all tests for statistical significance. ANCOVA, simple linear regression and correlation analyses were conducted using SPSS 23. The Bayesian mixing model using package simmr was conducted in R statistical software 3.5.1. Additional details on data analyses were provided in the Supporting Information.

3. Results and discussion

3.1. $\delta^{15}N$ of phenylalanine, glutamate, and bulk tissue

In the present study, we focused on the use of the two canonical amino acids for the TP_{AA} estimation: glutamate and phenylalanine. The $\delta^{15}N_{Phe}$ among the investigated samples ranged from 4.8 ± 0.4‰ to 16.1 ± 2.0‰ (Table 1), with the highest values in aquatic macrophytes and the lowest values in algae. These results are consistent with the general finding that the catabolism pathways of phenylalanine in algae and vascular plants were distinct (Styring et al., 2014). In vascular plants, the significant role of phenylalanine in the phenylpropanoid pathways for the biosynthesis of lignin and phenolic compounds was responsible for the relative ^{15}N-enrichment due to an enzymatic kinetic isotopic effect (i.e., the cleavage of C—N bonds) (Styring et al., 2014). The $\delta^{15}N_{Phe}$ in all consumers fell between the two dietary groups (Fig. 1). The lower $\delta^{15}N_{Phe}$ values were observed in filter-feeding consumers, such as silver carp (*Hypophthalmichthys nobilis*) and bighead carp (*Hypophthalmichthys molitrix*), which were very close to that of POM. On the other hand, the $\delta^{15}N_{Phe}$ in the herbivorous grass carp (*Ctenopharyngodon idellus*) were higher and close to that of aquatic macrophytes. These results are consistent with previous reports that the signature of phenylalanine is potentially useful for identifying the basal diet resources of a consumer (Choi et al., 2017). The $\delta^{15}N_{Glu}$ and $\delta^{15}N_{Bulk}$ displayed significant variations, ranging from 2.3 ± 1.0‰ (terrestrial input) to 27.7 ± 2.1‰ (whitebait), and from 5.6 ± 0.5‰ (algae) to 18.9 ± 0.8‰ (grenadier anchovy), respectively (Table 1). This large enrichment of $\delta^{15}N_{Glu}$ was consistent with the theory that consumers tended to be ^{15}N-enriched (+8.0‰) during each trophic stepwise because the metabolism of glutamate is dominated by transamination or deamination which highly favors ^{14}N via kinetic isotopic fractionation (Yamaguchi et al., 2017). In addition, the strong positive relationship between $\delta^{15}N_{Glu}$ and $\delta^{15}N_{Bulk}$ in biota ($R^2 = 0.71$, $p < 0.01$, Fig. S2) indicated a similar ability to predict TP.

3.2. Comparison between TP_{Bulk} and TP_{AA}

The TP_{AA} of Poyang Lake biota ranged from 1.0 ± 0.1 (primary producers) to 3.7 ± 0.2 (snakehead and whitebait, Table 1). In contrast, the highest TP_{Bulk} was 4.4 ± 0.1 for grenadier anchovy (Table S1), which was significantly higher than the corresponding TP_{AA} (3.0 ± 0.2). In general, the TP_{Bulk} was higher than TP_{AA} for most species (approximately 0.3–1.4 units; Fig. S3, Table 1, and Table S1). Such a discrepancy between the two approaches was observed previously (Ek et al., 2018; Kobayashi et al., 2019). For example, Kobayashi et al. (2019) reported that TP_{Bulk} (from 1.0–4.0 ± 0.1) tended to be larger than TP_{AA} values (from 1.0–3.5 ± 0.4) of food-web organisms in Tokyo Bay (Kobayashi et al., 2019). In the present study, planktivores (e.g, grenadier anchovy, saury fish, and stone moroko) showed TP_{AA} of 2.8 ± 0.2–3.0 ± 0.2, but their TP_{Bulk} values were generally higher than 3.5. In addition, shrimp (*Macrobranchium nipponense*) known to be omnivores was more reliably predicted by TP_{AA} (2.5 ± 0.2) rather than by TP_{Bulk} (3.4 ± 0.2). Compared with TP_{Bulk}, we suggested that TP_{AA} may serve as a more reliable estimation for the Poyang Lake organisms. Therefore, the aquatic food web structure of Poyang lake was illustrated using TP_{AA}, as presented in Fig.1. Generally, species known as primary producers, herbivores, and planktivores had well-understood trophic tendencies, as suggested by their integer TP_{AA} values (Chikaraishi et al., 2014). For instance, primary producers (e.g., aquatic macrophytes, algae, and terrestrial input) showed TP_{AA} values of near 1.0 (0.9–1.2); Snails, which fed primarily on algae and aquatic macrophytes, showed TP_{AA} of 1.9 ± 0.1; Herbivorous fish (grass carp and bream) showed TP_{AA} values of 2.0–2.2 (2.0 ± 0.2); Secondary consumers such as planktivores and crayfish showed TP_{AA} values near 3.0. Omnivores such as shrimps and benthic bivalves showed intermediate TP_{AA} values of 2.2–2.6, and carnivorous species (i.e., snakehead, catfish) had the highest TP_{AA} of 3.3

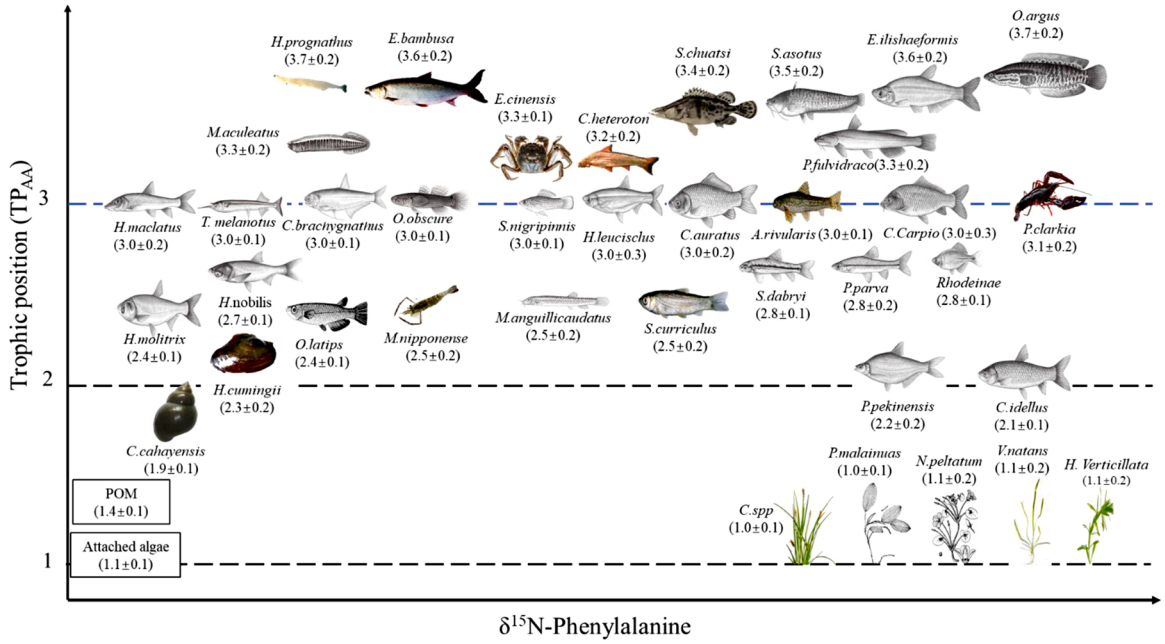

Fig. 1. Illustration of the aquatic food web structure of Poyang Lake ecosystems based on the CSIA-AA approach (TP_{AA}). Mean TP_{AA} values and 1SD for each species are shown in parenthesis near each organism. The *x*-axis represents the relative of $\delta^{15}N_{Phe}$ values in organisms. A detailed description of these freshwater species can be found in Table 1 and Table S1.

to 3.7. The predicted TP_{AA} of organisms in Poyang Lake were generally consistent with their known dietary habits.

3.3. THg and MeHg in the lake food web organisms

As in other studies, THg and MeHg concentrations of organisms in Poyang Lake varied significantly, from 0.84 (attached algae, n = 1) to 572 ± 134 ng/g (catfish, n = 5) and 0.17 (attached algae) to 517 ± 97 ng/g (catfish), respectively (Table 1). The levels of THg and MeHg of investigated organisms were roughly within the same order of magnitude as in other freshwater ecosystems of China (Jin et al., 2006; Li et al., 2010). MeHg concentrations and MeHg percentage (the proportion of THg as MeHg, ranged from 3.4%–98.5%) increased considerably from primary producers through herbivores to carnivorous fish species, similar to the pattern observed for TP_{AA} (Table 1, Fig. 2A and Fig. S4). The inorganic Hg (IHg) calculated by THg minus MeHg showed no obvious correlation with TP_{AA}, indicating limited IHg bioaccumulation potential along with the aquatic food web (Fig. S5). These results suggested that MeHg was the species to be efficiently biomagnified and bioaccumulated through food webs. For instance, an increased pattern (in "S" curve) of MeHg percentage was observed from primary producers (< 10 %), herbivores (12 %), primary consumers and omnivores (approximately 30%–80%) to planktivores and carnivorous fish (> 90 %), consistent with many previous studies (Fox et al., 2017; Van der Velden et al., 2013) (Fig. S4). The similar trends of MeHg concentrations and MeHg percentage with TP_{AA}, supported bioaccumulation of MeHg in Poyang aquatic food web and implied that MeHg concentrations and MeHg percentage in organisms can be alternative indicators of the TP.

3.4. TMF calculated using bulk and CSIA-AA approach

After being Log-transformed, the concentrations of MeHg were strongly and linearly correlated with TP_{Bulk} and TP_{AA} values ($R^2 = 0.72$ and 0.66, respectively, $p < 0.01$, Fig. 2). The TMF of MeHg based on TP_{Bulk} and TP_{AA} was estimated to be 5.7 ± 0.4 and 9.5 ± 0.5, respectively, which were within the range of global reviewed values for freshwater ecosystems based on bulk $\delta^{15}N$ method (8.3 ± 7.5) (Lavoie et al., 2013). However, the difference between the slopes of the relationship between Log MeHg with TP_{Bulk} or TP_{AA} was significant (ANCOVA, $F_{1,128} = 43.6$, $p < 0.001$). One of the possible reasons was the longer food chain length calculated using $\delta^{15}N_{Bulk}$ than the CSIA-AA approach (highest TP of 4.4 ± 0.1 vs 3.7 ± 0.2, respectively).

3.5. Amino acids composition

The basic profiles of AA composition among freshwater species in this study were similar (Fig. S6). Glutamate was the most abundant AA, followed by aspartate, alanine, lysine, glycine, leucine, and valine, while the sulfur-containing amino acids (cysteine, cystine, and methionine) were the lowest among the remaining AAs.

In general, the protein and individual AA contents showed considerable variability and were significantly and positively related to the TP_{AA} values across all species in the food webs (Pearson, $r = 0.27 \sim 0.70$, $p < 0.01$, Table S2, Fig. S7). For instance, the lowest levels of protein content were observed in primary producers (approximately 573 ± 33 and 1025 ± 74 nmol/mg for algae and terrestrial input, respectively, $TP_{AA} = 1.0 \pm 0.1$), while the highest concentrations observed in spotted steed (6641 ± 115 nmol/mg, $TP_{AA} = 3.0 \pm 0.2$, Table 1). Levels of cysteine were lowest in the primary producers (5.8 ± 0.7 for algae and 6.4 ± 1.1 for POM, respectively) and highest in the top predators (97.1 ± 3.8 and 99.0 ± 9.3 nmol/mg for snakehead and catfish, respectively), and generally followed the TP_{AA} ($R^2 = 0.49$, $p < 0.01$, Fig. S7 A). As with cysteine, other AAs also presented positive regressions with TP_{AA} (Table S2). However, there was no obvious correlation between TP_{AA} and protein or individual AA when primary

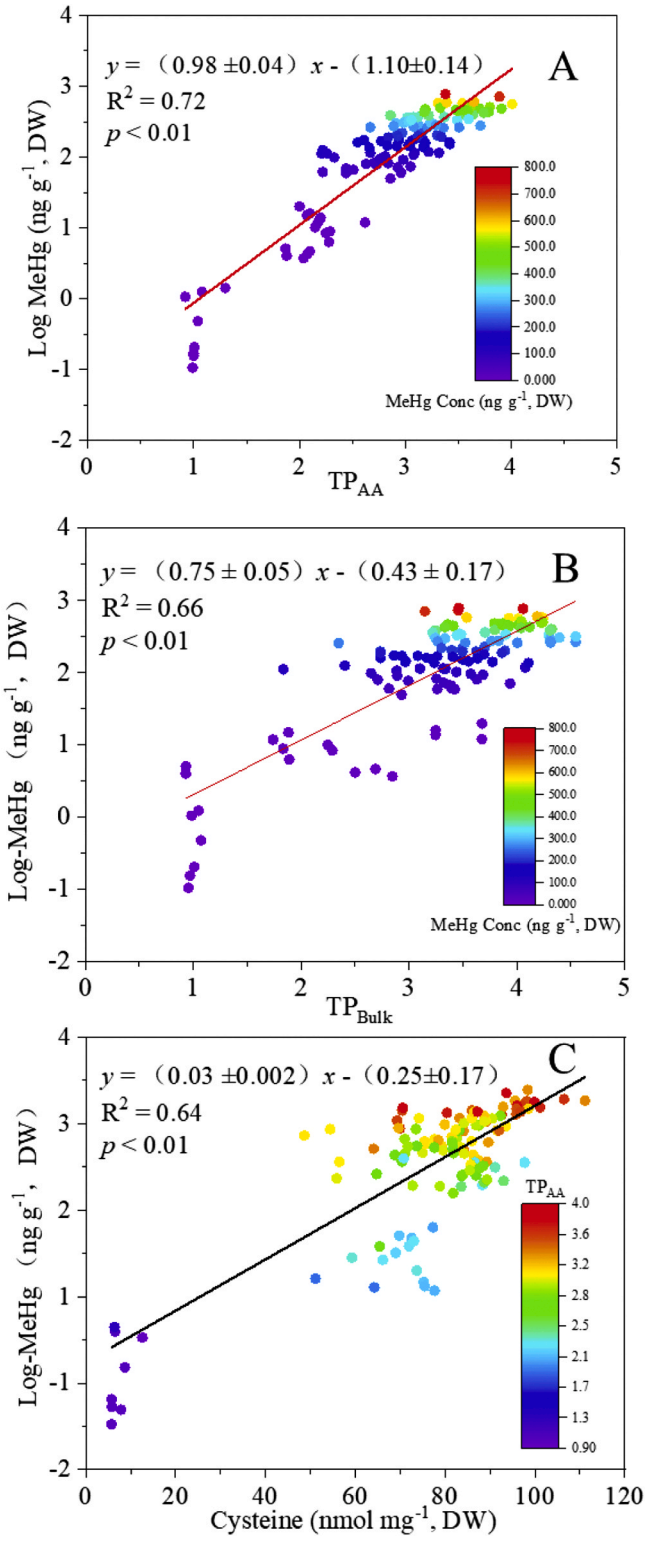

Fig. 2. Log-transformed MeHg (ng g^{-1}, DW) versus TP_{AA} (A), TP_{Bulk} (B) and cysteine concentrations (C, nmol g^{-1}, DW) of biota from Poyang Lake.

producers were excluded ($p > 0.05$, Table S3), except for cysteine ($R = 0.392$, $p < 0.01$, Table S3, Fig. S7 C). The bioaccumulation of cysteine through the food webs may be linked to its role in the storage of the sulfhydryl-reactive metals (i.e, cadmium, lead, mercury, and arsenic; Quig, 1998). For instance, the affinity constant for Hg binding to thiol anions (-SH) is in the order of magnitude of 10^{15} to 10^{20}, and cysteine is the only amino acid containing a free -SH group among the 19 primary

amino acids (Zalups, 2000; Zhang et al., 2004).

3.6. Effect of cysteine on the biomagnification of MeHg

Significant and positive linear regressions between Log-MeHg ($R^2 = 0.64$, $p < 0.01$) or Log-THg ($R^2 = 0.55$, $p < 0.01$) and cysteine were observed for all the samples (Fig. 2C, Fig. S8), respectively, suggesting that cysteine contents explained 55 % and 64 % of the variability of Log-THg and Log-MeHg. For instance, MeHg content of catfish ($TP_{AA} = 3.5 \pm 0.2$, MeHg = 517 ± 97 ng/g) tended to be higher than whitebait ($TP_{AA} = 3.7 \pm 0.2$, MeHg = 462 ± 28 ng/g), which may be partially explained by the higher cysteine concentration (99.0 ± 9.3 and 70.5 ± 0.7 nmol/mg for catfish and whitebait, respectively). We infer that the regression between MeHg and cysteine is driven by the formation of the MeHg-cysteine complex in organism tissue. In fact, MeHg is thought to be predominately conjugated with cysteine in fish muscle tissue (Dang and Wang, 2010; Harris et al., 2003), and the cycling of MeHg (i.e., storage, uptake, transport, distribution) also linked to the cysteine metabolism (Thera et al., 2019).

The previous study observed that a combination of cysteine and $\delta^{15}N_{Bulk}$ significantly predicted the MeHg contents of aquatic invertebrates (Thera et al., 2019). In contrast, the present study indicated cysteine combined with TP_{AA} can explain more variability in Log-MeHg through the food web than other combinations or individual variables (Text S5 and Table S4). For instance, the prediction models of Log-MeHg levels by $\delta^{15}N_{Bulk}$ with cysteine or protein were similar ($R^2_{adj} = 0.71$ and 0.70, AICc = -243 and -236, respectively), while the best one included cysteine with TP_{AA}, which accounted for more than 80 % of the variability in Log-MeHg ($R^2_{adj} = 0.86$, AICc = −324, Akaike weight accounted for 0.997). The increase in the model's prediction (R^2_{adj} up to 0.16, ΔAICc > -80) may be attributed to the accurate estimations of TP based on the CSIA-AA approach. Results further indicated that cysteine can account, to some extent, for the variability of MeHg in food web organisms. The cysteine levels were positively correlated with their corresponding TP_{AA} values ($R^2 = 0.49$, Fig. S7 A). Therefore, the relative importance of cysteine and TP to the food web transfer of MeHg is difficult to assess given the potential collinearity of these variables, although the VIF of cysteine with TP_{AA} less than 2.0 (Table S4). In brief, the trophic transfer process of MeHg through the food web is also linked to the bioaccumulation of cysteine, to which the MeHg is conjugated (Clayden et al., 2013; Harris et al., 2003; Leaner and Mason, 2002; Lemes and Wang, 2009; Schaefer and Morel, 2009; Simmons-Willis et al., 2002; Thera et al., 2019; Zhang et al., 2004). When the MeHg concentrations were normalized to cysteine or protein concentrations, the Log_{10} [MeHg: cysteine] or [MeHg: protein] ratios were found to be significantly and linearly correlated with TP_{AA} values, with a slope of 0.84 and 0.92 ($p < 0.01$, Fig. 3 B and C), respectively. The TMF_{AA} normalized with cysteine or protein contents was 6.9 ± 0.4 and 8.7 ± 0.5, respectively, for all the samples. Given that MeHg is primarily bound with subcellular heat-stable proteins (Dang and Wang, 2010) and conjugated with cysteine (Harris et al., 2003), the TMF_{AA} should be close to the original TMF value (9.5 ± 0.5). However, our TMF_{AA} values were lower than the original TMF values (slopes were compared using ANCOVA, $p < 0.01$).

A worldwide meta-analysis suggested that Hg in organisms at upper TP across ecosystems was primarily defined at primary consumer taxa (TP = 2), rather than primary producer (Lavoie et al., 2013). We, therefore, further examined the TMF for MeHg (without normalization, and normalized with cysteine or protein contents) after excluding the data of primary producers to clarify their influence on the regression. As a result, we observed similar TMF values among the three scenarios (8.7, 7.8, and 8.5, respectively), which indicated that the bioavailability of MeHg among consumers (TP ≥ 2) was comparable (Fig. 3). Our result was reasonable since earlier studies showed that most of the MeHg in fish was presented as MeHg-cysteine complex (> 90 %), and primarily distributed in the protein pool with an assimilation efficiency > 90 % (Dang and Wang, 2010). Our results also suggested that the MeHg contents should be normalized by cysteine or protein content to obtain the true TMF analysis (Burkhard et al., 2013).

4. Conclusion

MeHg biomagnifies with increasing trophic levels of the food web in an exponential manner, however, the mechanism underlying this

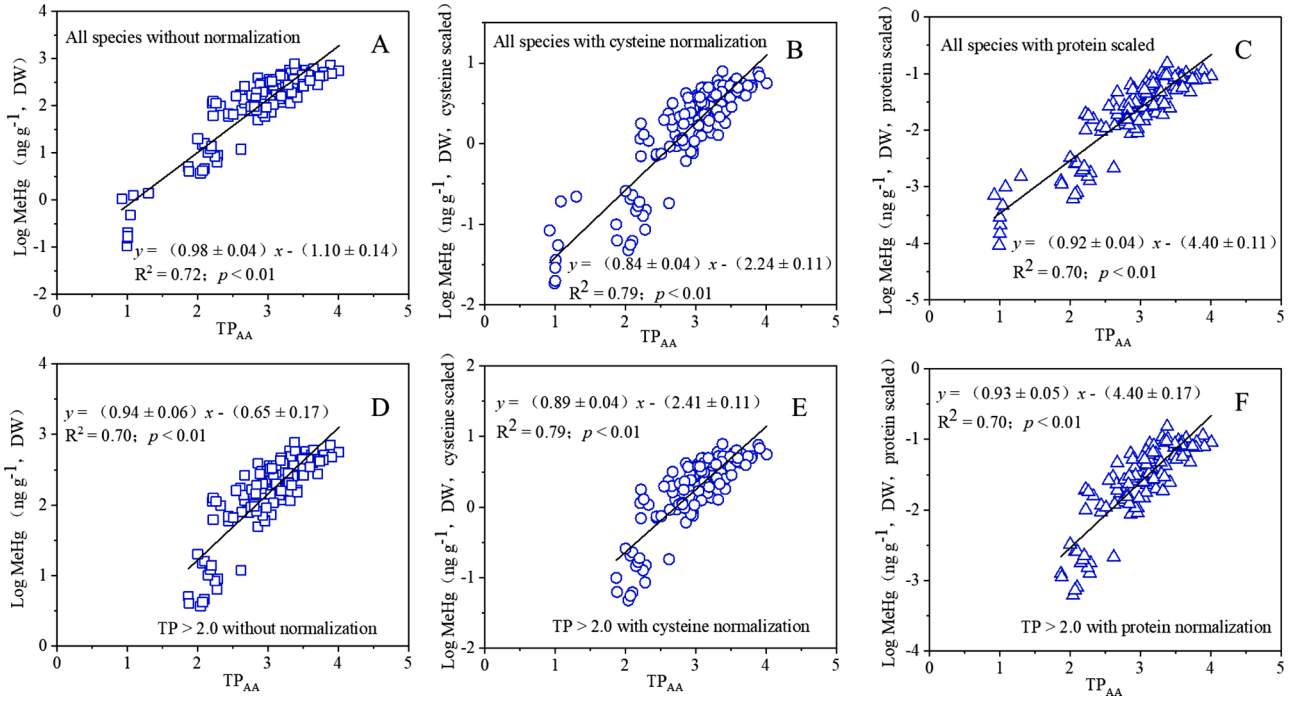

Fig. 3. Relationships between the Log-transformed MeHg concentrations (A), MeHg normalized by cysteine (B), or protein (C) against the trophic position (TP_{AA}) of all organisms. D, E, and F represent the relationships of Log-transformed MeHg concentrations, normalized by cysteine or protein against the consumers (TP ≥ 2).

scenario has not been well explained. In the present study, the trophic positions of investigated organisms in Poyang Lake, the largest freshwater lake of China, were determined using the CSIA-AA approach and contrasted with the traditional $\delta^{15}N_{Bulk}$ method. Results shown that the TP_{AA} of the organisms ranged from 1.0 ± 0.1–3.7 ± 0.2, generally consistent with their known ecologically trait. The TMF of MeHg along with the Poyang lake food webs was estimated to be 9.5 ± 0.5, similar to the global reviewed values of freshwater ecosystems. To our knowledge, the novel study represents the first interpretation of the importance of cellular medium (i.e., cysteine or protein) in MeHg biomagnification in a full food web. The TMFs of MeHg calculated with and without cysteine (or protein) normalization were comparable (7.7∼8.7) when excluding primary producers. Our results suggest that the formation of MeHg-cysteine serves as an important driving force of MeHg biomagnification through food webs. Although previous studies have suggested that the majority of MeHg in organisms is conjugated with cysteine, there is a lack of studies regarding the relationship between cysteine and MeHg across a full food web. We speculate that the metabolism of amino acids (especially cysteine) during trophic transfer may concentrate MeHg in protein to high trophic levels, leading to higher MeHg concentration and MeHg/cysteine or MeHg/protein ratios.

Declaration of Competing Interest

The authors declare no competing interests.

CRediT authorship contribution statement

Zhongyi Zhang: Conceptualization, Software, Investigation, Writing - original draft. **Wen-Xiong Wang:** Funding acquisition, Supervision, Validation, Writing - review & editing. **Nengjian Zheng:** Resources, Writing - review & editing, Data curation. **Yansheng Cao:** Resources, Writing - review & editing, Data curation. **Hongwei Xiao:** Methodology, Resources, Writing - review & editing, Data curation. **Renguo Zhu:** Methodology, Resources, Writing - review & editing, Data curation. **Hui Guan:** Conceptualization, Software, Investigation, Writing - original draft. **Huayun Xiao:** Funding acquisition, Project administration, Supervision, Validation, Writing - review & editing.

Acknowledgments

This study was supported by the National Natural Science Foundation of China (grants 41425014 and 41863001) and the Hong Kong Branch of Southern Marine Science and Engineering Guangdong Laboratory (Guangzhou) (SMSEGL20SC01).

Appendix A. Supplementary data

Supplementary material related to this article can be found, in the online version, at doi:https://doi.org/10.1016/j.jhazmat.2020.123700.

References

Abeysinghe, K.S., Qiu, G., Goodale, E., Anderson, C.W., Bishop, K., Evers, D.C., Goodale, M.W., Hintelmann, H., Liu, S., Mammides, C., 2017. Mercury flow through an Asian rice-based food web. Environ. Pollut. 229, 219–228.

Adediran, G.A., Liem-Nguyen, V., Song, Y., Schaefer, J.K., Skyllberg, U., Bjorn, E., 2019. Microbial biosynthesis of thiol compounds: implications for speciation, cellular uptake, and methylation of Hg(II). Environ. Sci. Tech. 53 (14), 8187–8196.

Anderson, D., Burnham, K., 2004. Model Selection and Multi-model Inference, 2nd ed. Springer-Verlag, NY, p. 63.

Blum, J.D., Popp, B.N., Drazen, J.C., Anela Choy, C., Johnson, M.W., 2013. Methylmercury production below the mixed layer in the North Pacific Ocean. Nat. Geosci. 6 (10), 879–884.

Borgå, K., Kidd, K.A., Muir, D.C.G., Berglund, O., Conder, J.M., Gobas, F.A.P.C., Kucklick, J., Malm, O., Powell, D.E., 2012. Trophic magnification factors: considerations of ecology, ecosystems, and study design. Integr. Environ. Asses. 8 (1), 64–84.

Burkhard, L.P., Borga, K., Powell, D.E., Leonards, P., Muir, D.C., Parkerton, T.F., Woodburn, K.B., 2013. Improving the quality and scientific understanding of trophic magnification factors (TMFs). Environ. Sci. Technol. 47 (3), 1186–1187.

Chikaraishi, Y., Ogawa, N.O., Kashiyama, Y., Takano, Y., Suga, H., Tomitani, A., Miyashita, H., Kitazato, H., Ohkouchi, N., 2009. Determination of aquatic food-web structure based on compound-specific nitrogen isotopic composition of amino acids. Limnol. Oceanogra: Met. 7 (11), 740–750.

Chikaraishi, Y., Steffan, S.A., Ogawa, N.O., Ishikawa, N.F., Sasaki, Y., Tsuchiya, M., Ohkouchi, N., 2014. High-resolution food webs based on nitrogen isotopic composition of amino acids. Ecol. Evol. 4 (12), 2423–2449.

Choi, B., Ha, S.-Y., Lee, J.S., Chikaraishi, Y., Ohkouchi, N., Shin, K.-H., 2017. Trophic interaction among organisms in a seagrass meadow ecosystem as revealed by bulk $\delta^{13}C$ and amino acid $\delta^{15}N$ analyses. Limnol. Oceanogra. 62 (4), 1426–1435.

Clayden, M.G., Kidd, K.A., Wyn, B., Kirk, J.L., Muir, D.C., O'Driscoll, N.J., 2013. Mercury biomagnification through food webs is affected by physical and chemical characteristics of lakes. Environ. Sci. Tech. 47 (21), 12047–12053.

Cummings, B.M., Schindler, D.E., 2013. Depth variation in isotopic composition of benthic resources and assessment of sculpin feeding patterns in an oligotrophic Alaskan lake. Aquat. Ecol. 47 (4), 403–414.

Dang, F., Wang, W.X., 2010. Subcellular controls of mercury trophic transfer to a marine fish. Aquat. Toxicol. 99 (4), 500–506.

Driscoll, C.T., Mason, R.P., Chan, H.M., Jacob, D.J., Pirrone, N., 2013. Mercury as a global pollutant: sources, pathways, and effects. Environ. Sci. Tech. 47 (10), 4967–4983.

Ek, C., Holmstrand, H., Mustajarvi, L., Garbaras, A., Bariseviciu Te, R.T., Sapolaite, J., Sobek, A., Gorokhova, E., Karlson, A.M.L., 2018. Using compound-specific and bulk stable isotope analysis for trophic positioning of bivalves in contaminated baltic sea sediments. Environ. Sci. Technol. 52 (8), 4861–4868.

EPA, U, 2002. Mercury in Water by Oxidation, Purge and Trap, and Cold Vapor Atomic Fluorescence Spectrometry. OW, EPA-821-R-02-019.

Fox, A.L., Trefry, J.H., Trocine, R.P., Dunton, K.H., Lasorsa, B.K., Konar, B., Ashjian, C.J., Cooper, L.W., 2017. Mercury biomagnification in food webs of the Northeastern Chukchi Sea, Alaskan Arctic. Deep. Sea. Res. Pt. II 144, 63–72.

Harris, H.H., Pickering, I.J., George, G.N., 2003. The chemical form of mercury in fish. Science 301 (5637), 1203-1203.

Hussey, N.E., Macneil, M.A., McMeans, B.C., Olin, J.A., Dudley, S.F., Cliff, G., Wintner, S. P., Fennessy, S.T., Fisk, A.T., 2014. Rescaling the trophic structure of marine food webs. Ecol. Lett. 17 (2), 239–250.

Jin, L., Liang, L., Jiang, G., Xu, Y., 2006. Methylmercury, total mercury and total selenium in four common freshwater fish species from Ya-Er Lake. China. Environ. Geochem. Hlth. 28 (5), 401–407.

Karimi, R., Chen, C.Y., Pickhardt, P.C., Fisher, N.S., Folt, C.L., 2007. Stoichiometric controls of mercury dilution by growth. Proc. Natl. Acad. Sci. U. S. A 104 (18), 7477–7482.

Kidd, K.A., Bootsma, H.A., Hesslein, R.H., Muir, D.C., Hecky, R.E., 2001. Biomagnification of DDT through the benthic and pelagic food webs of Lake Malawi, East Africa: importance of trophic level and carbon source. Environ. Sci. Tech. 35 (1), 14–20.

Kobayashi, J., Yoshimoto, M., Yamada, K., Okamura, K., Sakurai, T., 2019. Comparison of trophic magnification factors of PCBs and PBDEs in Tokyo Bay based on nitrogen isotope ratios in bulk nitrogen and amino acids. Chemosphere 226, 220–228.

Lavoie, R.A., Jardine, T.D., Chumchal, M.M., Kidd, K.A., Campbell, L.M., 2013. Biomagnification of mercury in aquatic food webs: a worldwide meta-analysis. Environ. Sci. Tech. 47 (23), 13385–13394.

Leaner, J.J., Mason, R.P., 2002. Factors controlling the bioavailability of ingested methylmercury to channel catfish and Atlantic Sturgeon. Environ. Sci. Tech. 36 (23), 5124–5129.

Lemes, M., Wang, F., 2009. Methylmercury speciation in fish muscle by HPLC-ICP-MS following enzymatic hydrolysis. J. Anal., Atom. Spectrom. 24 (5), 663.

Lescord, G.L., Johnston, T.A., Branfireun, B.A., Gunn, J.M.J.Et., 2018. Percentage of methylmercury in the muscle tissue of freshwater fish varies with body size and age and among species. Environ. Toxi. Chem. 37 (10), 2682–2691.

Li, P., Feng, X., Qiu, G., 2010. Methylmercury exposure and health effects from rice and fish consumption: a review. Int. J. Env. Res. Pub. He 7 (6), 2666–2691.

Li, M., Schartup, A.T., Valberg, A.P., Ewald, J.D., Krabbenhoft, D.P., Yin, R., Balcom, P. H., Sunderland, E.M., 2016. Environmental origins of methylmercury accumulated in subarctic estuarine fish indicated by mercury stable isotopes. Environ. Sci. Tech. 50, 11559–11568.

Liang, L.-N., Jiang, G.-B., Liu, J.-F., Hu, J.-T., 2003. Speciation analysis of mercury in seafood by using high-performance liquid chromatography on-line coupled with cold-vapor atomic fluorescence spectrometry via a post column microwave digestion. Anal. Chim. Acta 477 (1), 131–137.

Lorrain, A., Graham, B.S., Popp, B.N., Allain, V., Olson, R.J., Hunt, B.P.V., Potier, M., Fry, B., Galván-Magaña, F., Menkes, C.E.R., Kaehler, S., Ménard, F., 2015. Nitrogen isotopic baselines and implications for estimating foraging habitat and trophic position of yellowfin tuna in the Indian and Pacific Oceans. Deep. Sea. Res. Pt. II 113, 188–198.

Man, Y., Yin, R., Cai, K., Qin, C., Wang, J., Yan, H., Li, M., 2019. Primary amino acids affect the distribution of methylmercury rather than inorganic mercury among tissues of two farmed-raised fish species. Chemosphere 225, 320–328.

Manneberg, M., Lahm, H.W., Fountoulakis, M., 1995. Quantification of cysteine residues following oxidation to cysteic acid in the presence of sodium azide. Anal. Biochem. 231 (2), 349.

Matthews, B., Mazumder, A., 2003. Compositional and interlake variability of zooplankton affect baseline stable isotope signatures. Limnol. Oceanogra. 48 (5), 1977–1987.

Mcmahon, K.W., Mccarthy, M.D., 2016. Embracing variability in amino acid $\delta^{15}N$ fractionation: mechanisms, implications, and applications for trophic ecology. Ecosphere 7 (12), e01511.
O'Connell, T.C., 2017. 'Trophic' and' source' amino acids in trophic estimation: a likely metabolic explanation. Oecologia 184 (2), 317–326.
Parnell, A.C., Phillips, D.L., Bearhop, S., Semmens, B.X., Ward, E.J., Moore, J.W., Jackson, A.L., Grey, J., Kelly, D.J., Inger, R., 2013. Bayesian stable isotope mixing models. Environmetrics 6 (24), 387–399.
Pirrone, N., Cinnirella, S., Feng, X., Finkelman, R.B., Friedli, H.R., Leaner, J., Mason, R., Mukherjee, A.B., Stracher, G.B., Streets, D.G., Telmer, K., 2010. Global mercury emissions to the atmosphere from anthropogenic and natural sources. Atmos. Chem. Phys. 10 (13), 5951–5964.
Post, D.M., 2002. Using stable isotopes to estimate trophic position: models, methods, and assumptions. Ecology 83 (3), 703–718.
Quig, D., 1998. Cysteine metabolism and metal toxicity. Altern. Med. Rev. 3 (4), 262–270.
Robbins, C.T., Felicetti, L.A., Florin, S.T., 2010. The impact of protein quality on stable nitrogen isotope ratio discrimination and assimilated diet estimation. Oecologia 162 (3), 571–579.
Ruus, A., Overjordet, I.B., Braaten, H.F., Evenset, A., Christensen, G., Heimstad, E.S., Gabrielsen, G.W., Borga, K., 2015. Methylmercury biomagnification in an Arctic pelagic food web. Environ. Toxicol. Chem. 34 (11), 2636–2643.
Sackett, D.K., Drazen, J.C., Choy, C.A., Popp, B., Pitz, G.L., 2015. Mercury sources and trophic ecology for Hawaiian bottomfish. Environ. Sci. Tech. 49 (11), 6909–6918.
Schaefer, J.K., Morel, F.M.M., 2009. High methylation rates of mercury bound to cysteine by Geobacter sulfurreducens. Nat. Geosci. 2 (2), 123–126.
Selin, N.E., 2009. Global biogeochemical cycling of mercury: a review. Annu. Rev. Env. Resour. 34, 43–63.
Simmons-Willis, T.A., Clarkson, T.W., Ballatori, N., 2002. Transport of a neurotoxicant by molecular mimicry: the methylmercury–L-cysteine complex is a substrate for human L-type large neutral amino acid transporter (LAT) 1 and LAT2. Biochem. J. 367 (1), 239–246.
Steffan, S.A., Chikaraishi, Y., Currie, C.R., Horn, H., Gaines-Day, H.R., Pauli, J.N., Zalapa, J.E., Ohkouchi, N., 2015. Microbes are trophic analogs of animals. Proc. Natl. Acad. Sci. U. S. A. 112 (49), 15119–15124.
Styring, A.K., Fraser, R.A., Bogaard, A., Evershed, R.P., 2014. Cereal grain, rachis and pulse seed amino acid delta15N values as indicators of plant nitrogen metabolism. Phytochem 97, 20–29.
Thera, J.C., Kidd, K.A., Bertolo, R.F., O'Driscoll, N.J., 2019. Tissue content of thiol-containing amino acids predicts methylmercury in aquatic invertebrates. Sci. Total Environ. 688, 567–573.
Van der Velden, S., Dempson, J., Evans, M., Muir, D., Power, M., 2013. Basal mercury concentrations and biomagnification rates in freshwater and marine food webs: effects on Arctic charr (Salvelinus alpinus) from eastern Canada. Sci. Total Environ. 444, 531–542.
Wang, W.-X., 2012. Biodynamic understanding of mercury accumulation in marine and freshwater fish. Adv. Environ. Res. 1, 15–35.
Yamaguchi, Y.T., Chikaraishi, Y., Takano, Y., Ogawa, N.O., Imachi, H., Yokoyama, Y., Ohkouchi, N., 2017. Fractionation of nitrogen isotopes during amino acid metabolism in heterotrophic and chemolithoautotrophic microbes across Eukarya, Bacteria, and Archaea: effects of nitrogen sources and metabolic pathways. Org. Geochem. 111, 101–112.
Yin, R., Feng, X., Zhang, J., Pan, K., Wang, W., Li, X., 2016. Using mercury isotopes to understand the bioaccumulation of Hg in the subtropical Pearl River Estuary, South China. Chemosphere 147, 173–179.
Yin, R., Zhang, W., Sun, G., Feng, Z., Hurley, J.P., Yang, L., Shang, L., Feng, X., 2017. Mercury risk in poultry in the Wanshan Mercury Mine. China. Environ. Pollut. 230, 810–816.
Zalups, R.K., 2000. Molecular interactions with mercury in the kidney. Pharmacol. Rev. 52 (1), 113–144.
Zanden, M.J.V., Rasmussen, J.B., 2001. Variation in $\delta^{15}N$ and $\delta^{13}C$ trophic fractionation: implications for aquatic food web studies. Limnol. Oceanogra. 46 (8), 2061–2066.
Zhang, J., Wang, F., House, J.D., Page, B., 2004. Thiols in wetland interstitial waters and their role in mercury and methylmercury speciation. Limnol. Oceanogr. 49 (6), 2276–2286.
Zhang, Z., Tian, J., Xiao, H., Zheng, N., Gao, X., Zhu, R., Xiao, H., 2016. A reliable compound-specific nitrogen isotope analysis of amino acids by GC-C-IRMS following derivatisation into N-pivaloyl-iso-propyl (NPIP)esters for high-resolution food webs estimation. J. Chromatogra. B 1033-1034, 382–389.
Zhang, Z., Tian, J., Cao, Y., Zheng, N., Zhao, J., Xiao, H., Guo, W., Zhu, R., Xiao, H., 2019. Elucidating food web structure of the Poyang Lake ecosystem using amino acid nitrogen isotopes and Bayesian mixing model. Limnol. Oceanogray: Met. 17, 555–564.
Zhu, R.G., Xiao, H.Y., Zhang, Z., Lai, Y., 2018. Compound-specific delta(^{15})N composition of free amino acids in moss as indicators of atmospheric nitrogen sources. Sci. Rep. 8 (1), 14347.